Electronic Supplementary Material (ESI) for Energy & Environmental Science.
This journal is © The Royal Society of Chemistry 2018

Supplementary Information for:

Enabling Alternative Ethylene Production through Its Selective Adsorption in the Metal–Organic Framework Mn_2(*m*-dobdc)

Jonathan E. Bachman, Douglas A. Reed, Matthew T. Kapelewski, Gaurav Chachra, Divya Jonnavittula, Guido Radaelli, and Jeffrey R. Long*

*email: jrlong@berkeley.edu

Breakthrough Simulation Model Configuration:

Material Balance Assumption: Plug flow without dispersion effects (convection only).

Momentum Balance Assumption: Gas velocity and pressure drop was represented by Ergun equation:

$$\frac{\partial P}{\partial z} = -\left(\frac{1.5 \times 10^{-3}(1-\varepsilon_i)^2}{\left(2r_p\psi\right)^2 {\varepsilon_i}^3}\mu v_g + 1.75 \times 10^{-5}\mathrm{M}\rho_g \frac{(1-\varepsilon_i)}{2r_p\psi{\varepsilon_i}^3}{v_g}^2\right)$$

Kinetic Model Assumption: Separate mass transfer resistances were lumped as a single overall factor:

$$\frac{\partial w_i}{\partial t} = MTC_{si}(w_i^* - w_i)$$

Isotherm Model: Dual site Langmuir Freundlich model, as fitted to the experimentally obtained equilibrium loading data, was used in the simulation:

$$w_i = \frac{IP_1 IP_2 P_i^{IP_3}}{1 + IP_1 IP_2 P_i^{IP_3}} + \frac{IP_4 IP_5 P_i^{IP_6}}{1 + IP_4 IP_5 P_i^{IP_6}}$$

Energy Balance: The simulation was set up to be isothermal since the experimental setup was kept under a water bath, to keep the system temperature to be nearly constant.

Numerical Method: First order upward differencing scheme was used as the numerical discretization method to solve the partial differential equations. The bed was divided in 20 nodes.

Supplementary Table 1. Dual-site Langmuir-Freundlich equation fits for CH_4, CO, and CO_2 in Mn_2(*m*-dobdc).

	CH_4			CO_2			CO		
T (°C)	25	35	45	25	35	45	25	35	45
$q_{sat,a}$ (mmol/g)	4.513	6.498	5.555	7.019	6.527	6.232	5.565	5.264	5.103
b_a (1/bar)	0.342	0.188	0.157	5.772	4.322	2.883	1.610	1.228	0.912
v_a	1.036	1.003	1.001	0.977	1.003	0.995	0.925	0.949	0.968
$q_{sat,b}$ (mmol/g)	0	0	0	3.491	3.244	3.099	0	0	0
b_b (1/bar)	n/a	n/a	n/a	0.280	0.274	0.281	n/a	n/a	n/a
v_b	n/a	n/a	n/a	1.761	1.404	1.088	n/a	n/a	n/a

Supplementary Table 2. Dual-site Langmuir-Freundlich equation fits for ethylene and ethane in Mn_2(*m*-dobdc)

	Ethylene			Ethane		
T (°C)	25	35	45	25	35	45
$q_{sat,a}$ (mmol/g)	5.603	5.451	5.421	6.854	7.727	6.700
b_a (1/bar)	73.02	48.25	30.43	6.228	4.080	2.606
v_a	0.854	0.868	0.876	1.170	1.173	1.153
$q_{sat,b}$ (mmol/g)	23.94	10.72	9.560	0	0	0
b_b (1/bar)	0.057	0.116	0.109	n/a	n/a	n/a
v_b	0.727	0.646	0.632	n/a	n/a	n/a

Supplementary Table 3. Dual-site Langmuir-Freundlich equation fits for CH_4, CO, and CO_2 in Fe_2(*m*-dobdc)

	CH_4			CO_2			CO		
T (°C)	25	35	45	25	35	45	25	35	45
$q_{sat,a}$ (mmol/g)	4.812	14.00	14.90	10.06	7.126	6.921	5.656	5.749	5.435
b_a (1/bar)	0.235	0.083	0.022	0.324	4.227	2.825	0.207	10.65	7.912
v_a	1.073	0.963	0.847	0.691	1.020	1.019	0.410	0.866	0.895
$q_{sat,b}$ (mmol/g)	9.740	0	0	4.723	1.606	1.540	4.842	0.794	1.125
b_b (1/bar)	0.044	n/a	n/a	11.25	0.336	0.342	29.03	0.233	0.343
v_b	0.843	n/a	n/a	1.138	1.885	1.477	0.967	1.405	1.079

Supplementary Table 4. Dual-site Langmuir-Freundlich equation fits for ethylene and ethane in Fe_2(*m*-dobdc)

	Ethylene			Ethane		
T (°C)	25	35	45	25	35	45
$q_{sat,a}$ (mmol/g)	5.657	5.288	5.479	4.907	4.250	3.485
b_a (1/bar)	59.52	48.99	28.01	9.727	6.895	4.924
v_a	0.735	0.771	0.776	1.254	1.295	1.344
$q_{sat,b}$ (mmol/g)	3.841	4.255	7.464	3.274	3.703	4.049
b_b (1/bar)	0.503	0.500	0.173	0.876	0.947	1.004
v_b	0.790	0.593	0.576	0.700	0.761	0.818

Supplementary Table 5. Dual-site Langmuir-Freundlich equation fits for CH_4, CO, and CO_2 in Co_2(*m*-dobdc)

	CH_4			CO_2			CO		
T (°C)	25	35	45	25	35	45	25	35	45
$q_{sat,a}$ (mmol/g)	9.874	9.035	8.270	7.162	3.286	2.354	6.078	3.614	3.324
b_a (1/bar)	0.182	0.157	0.137	10.21	14.20	9.258	71.42	94.97	85.06
v_a	0.990	0.998	0.999	1.041	1.214	1.249	0.877	0.953	0.996
$q_{sat,b}$ (mmol/g)	0	0	0	2.079	5.354	5.958	0.909	2.659	2.868
b_b (1/bar)	n/a	n/a	n/a	0.370	1.822	1.816	0.207	13.46	10.94
v_b	n/a	n/a	n/a	2.357	0.841	0.889	0.878	0.807	0.918

Supplementary Table 6. Dual-site Langmuir-Freundlich equation fits for ethylene and ethane in Co_2(*m*-dobdc)

	Ethylene			Ethane		
T (°C)	25	35	45	25	35	45
$q_{sat,a}$ (mmol/g)	5.968	5.983	5.850	5.756	3.409	0.178
b_a (1/bar)	79.89	45.60	29.82	8.88	0.362	82.65
v_a	0.869	0.866	0.876	1.133	0.707	2.270
$q_{sat,b}$ (mmol/g)	4.917	9.454	3.615	3.724	5.561	6.697
b_b (1/bar)	0.293	0.108	0.321	0.362	5.767	2.725
v_b	0.838	0.760	0.719	0.684	1.130	1.033

Supplementary Table 7. Dual-site Langmuir-Freundlich equation fits for CH_4, CO, and CO_2 in Ni_2(*m*-dobdc)

	CH_4			CO_2			CO		
T (°C)	25	35	45	25	35	45	25	35	45
$q_{sat,a}$ (mmol/g)	9.215	8.715	8.335	5.763	5.872	6.072	4.750	5.538	4.083
b_a (1/bar)	0.199	0.165	0.137	29.39	16.74	9.459	217.3	59.31	87.44
v_a	0.996	1.011	1.010	1.036	1.024	1.017	0.879	0.784	0.869
$q_{sat,b}$ (mmol/g)	0	0	0	3.796	1.706	1.679	1.084	0.224	1.577
b_b (1/bar)	n/a	n/a	n/a	0.489	0.942	0.400	6.149	6.924	14.01
v_b	n/a	n/a	n/a	1.357	1.692	2.037	0.617	2.105	0.910

Supplementary Table 8. Dual-site Langmuir-Freundlich equation fits for ethylene and ethane in Ni_2(*m*-dobdc).

	Ethylene			Ethane		
T (°C)	25	35	45	25	35	45
$q_{sat,a}$ (mmol/g)	5.496	5.304	5.631	6.666	6.510	6.321
b_a (1/bar)	52.14	38.07	21.79	6.824	4.804	3.460
v_a	0.755	0.777	0.776	1.046	1.063	1.075
$q_{sat,b}$ (mmol/g)	5.558	6.990	1.003	0	0	0
b_b (1/bar)	0.267	0.192	1.784	n/a	n/a	n/a
v_b	0.866	0.727	1.774	n/a	n/a	n/a

Supplementary Table 9. Dual-site Langmuir-Freundlich equation fits for CH_4, CO, and CO_2 in zeolite CaX.

	CH_4			CO_2			CO		
T (°C)	25	35	45	25	35	45	25	35	45
$q_{sat,a}$ (mmol/g)	2.761	2.532	1.933	6.011	6.573	7.009	1.275	1.256	1.290
b_a (1/bar)	0.302	0.281	0.299	3.211	2.047	1.380	0.923	0.817	0.670
v_a	0.876	0.902	0.936	0.674	0.620	0.597	1.088	1.037	0.991
$q_{sat,b}$ (mmol/g)	n/a	n/a	n/a	0.485	0.285	0.203	0.568	0.480	0.410
b_b (1/bar)	n/a	n/a	n/a	1522	1573	1466	23.91	21.84	17.00
v_b	n/a	n/a	n/a	1.326	1.233	1.265	0.933	0.977	1.007

Supplementary Table 10. Dual-site Langmuir-Freundlich equation fits for ethylene and ethane in zeolite CaX.

	Ethylene			Ethane		
T (°C)	25	35	45	25	35	45
$q_{sat,a}$ (mmol/g)	2.845	3.353	3.873	2.858	0.348	0.327
b_a (1/bar)	2.498	2.040	1.701	3.793	0.079	0.074
v_a	0.604	0.534	0.477	1.269	0.481	0.672
$q_{sat,b}$ (mmol/g)	1.051	0.644	0.287	0.377	4.198	4.460
b_b (1/bar)	28.59	52.25	1488	42.10	1.301	0.904
v_b	0.477	0.513	0.848	0.979	0.861	0.860

Supplementary Table 11. Mass transfer coefficients used in breakthrough simulations.

Gas	Value
Ethylene	0.0125 s^{-1}
Ethane	0.0037 s^{-1}
CO_2	0.01 s^{-1}
CO	0.0125 s^{-1}
Methane	0.004 s^{-1}

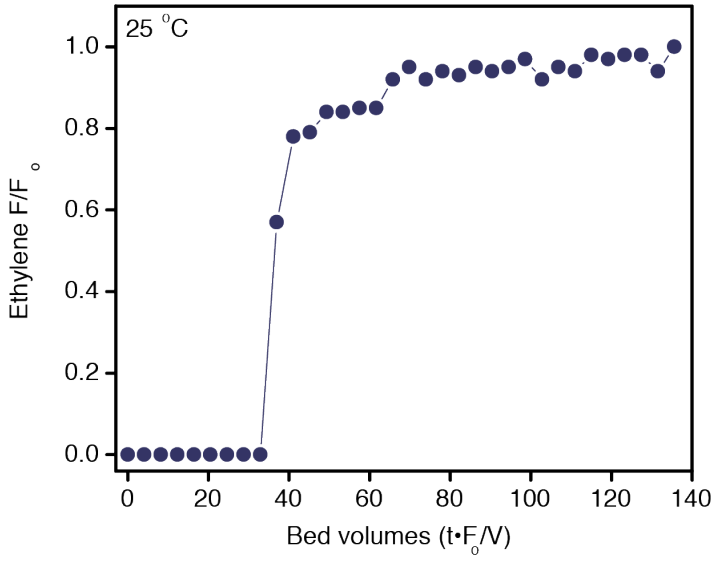

Supplementary Figure 1. Single-component transient breakthrough curve of ethylene in Mn_2(*m*-dobdc). Breakthrough capacity was determined to be 6.81 mmol/g.

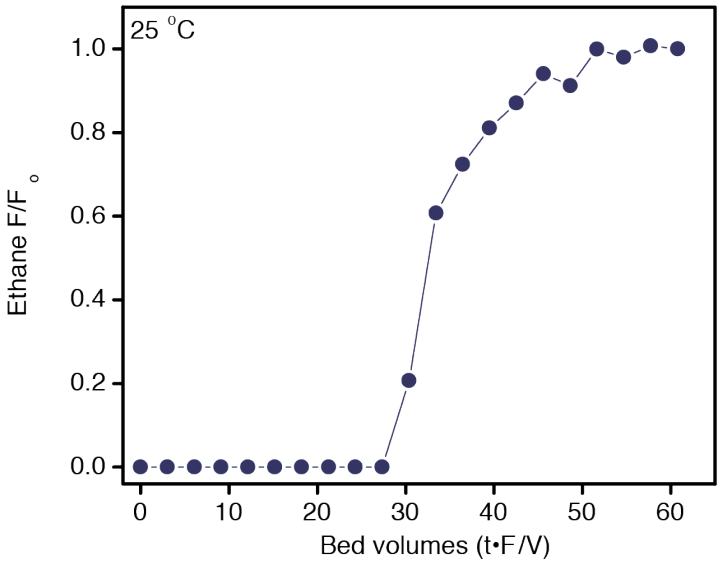

Supplementary Figure 2. Single-component transient breakthrough curve of ethane in Mn_2(*m*-dobdc). Breakthrough capacity was determined to be 6.31 mmol/g.

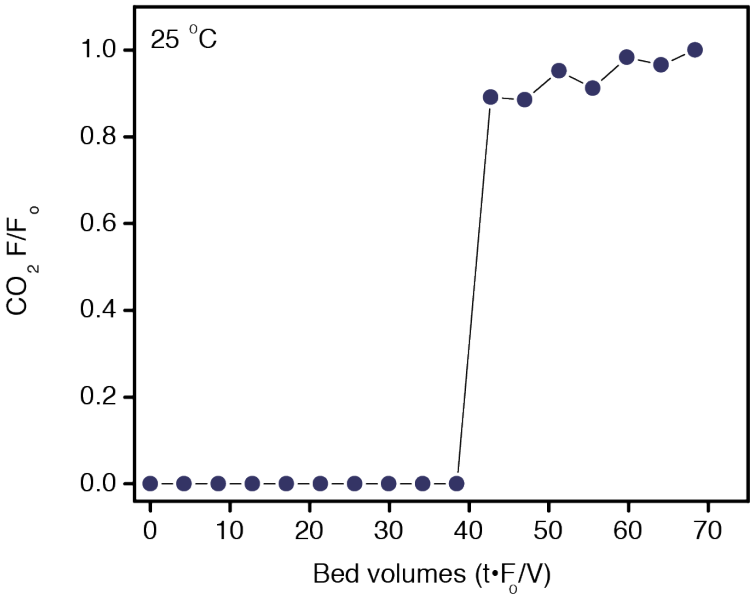

Supplementary Figure 3. Single-component transient breakthrough curve of CO_2 in Mn_2(*m*-dobdc). Breakthrough capacity was determined to be 4.67 mmol/g.

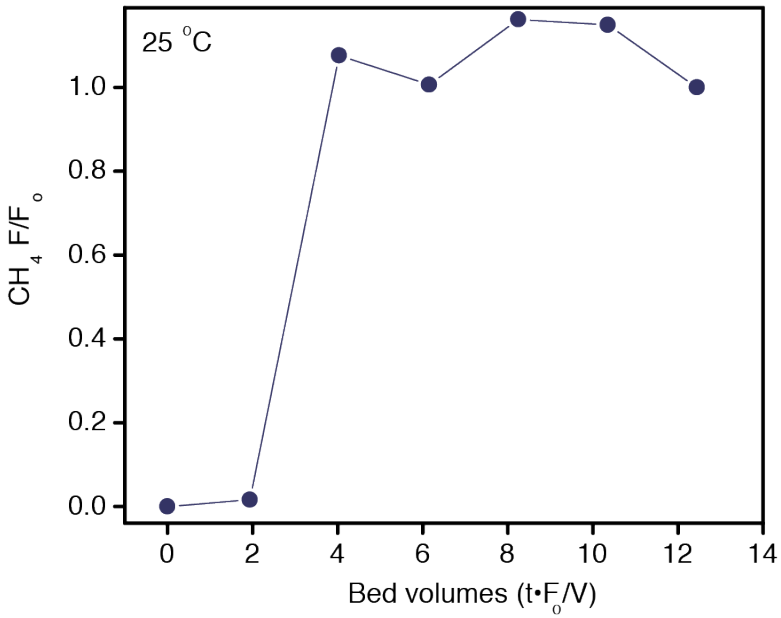

Supplementary Figure 4. Single-component transient breakthrough curve of CH_4 in Mn_2(*m*-dobdc). Breakthrough capacity was determined to be 0.09 mmol/g.

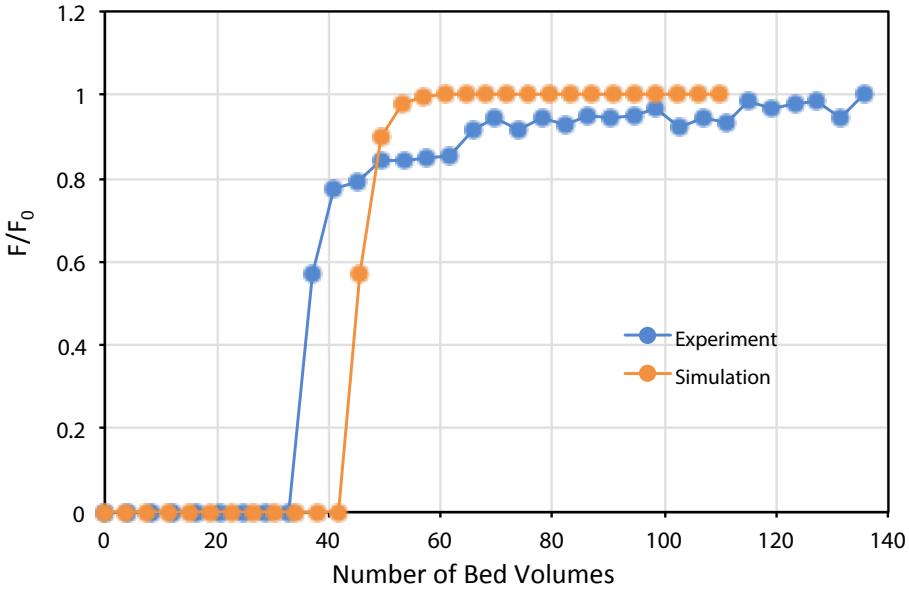

Supplementary Figure 5. Single component ethylene breakthrough simulation and experiment. Simulations were performed using experimentally determined equilibrium isotherms and mass transfer coefficients were fit to match the breakthrough curve.

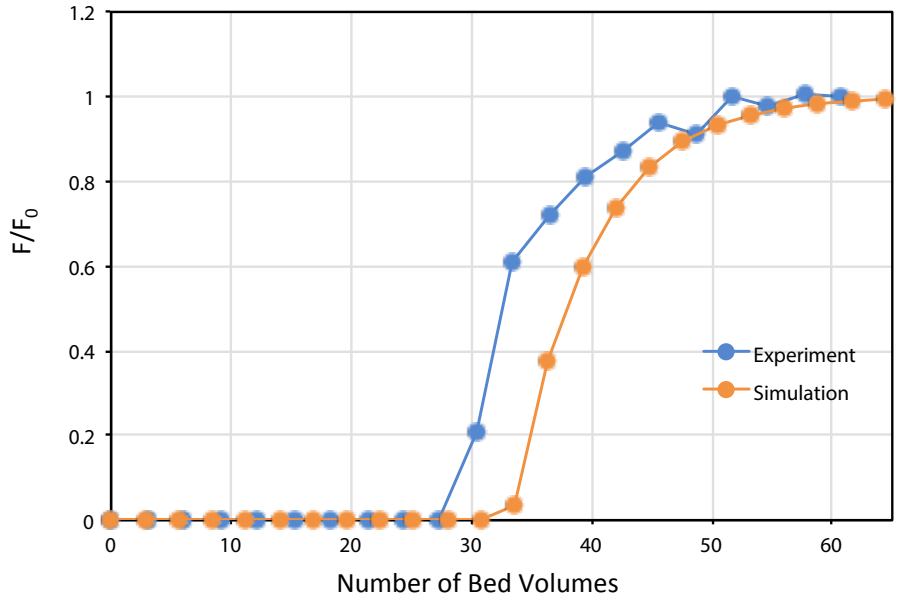

Supplementary Figure 6. Single component ethane breakthrough simulation and experiment. Simulations were performed using experimentally determined equilibrium isotherms and mass transfer coefficients were fit to match the breakthrough curve.

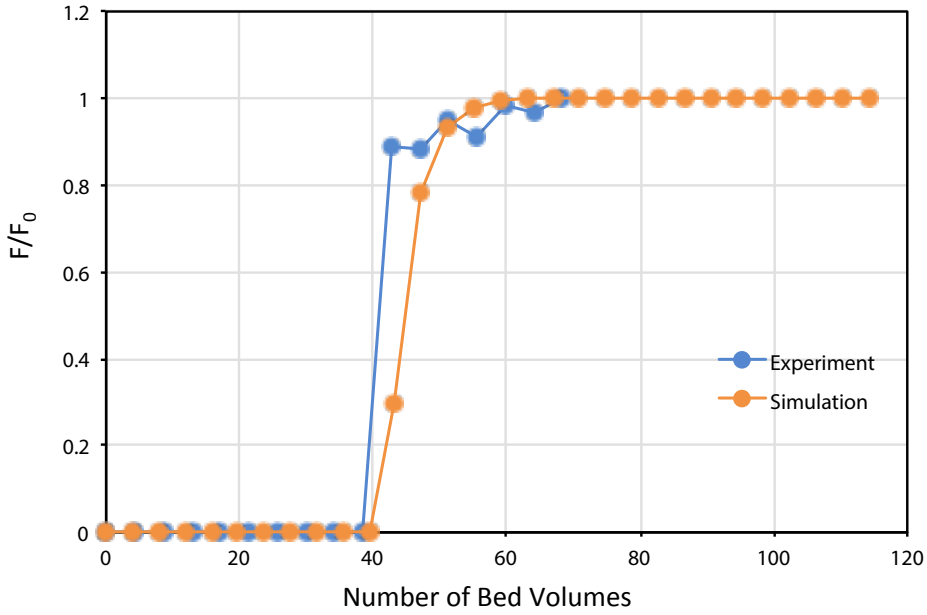

Supplementary Figure 7. Single component CO_2 breakthrough simulation and experiment. Simulations were performed using experimentally determined equilibrium isotherms and mass transfer coefficients were fit to match the breakthrough curve.

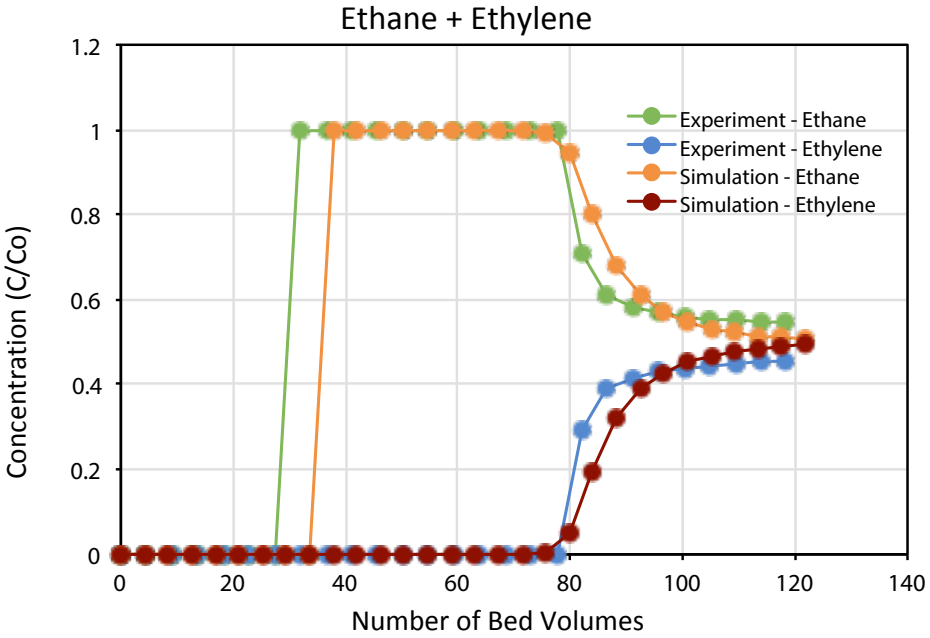

Supplementary Figure 8. Binary equimolar ethylene/ethane breakthrough simulation and experiment. Simulations were performed using experimentally determined equilibrium isotherms and mass transfer coefficients obtained from single-component breakthrough.

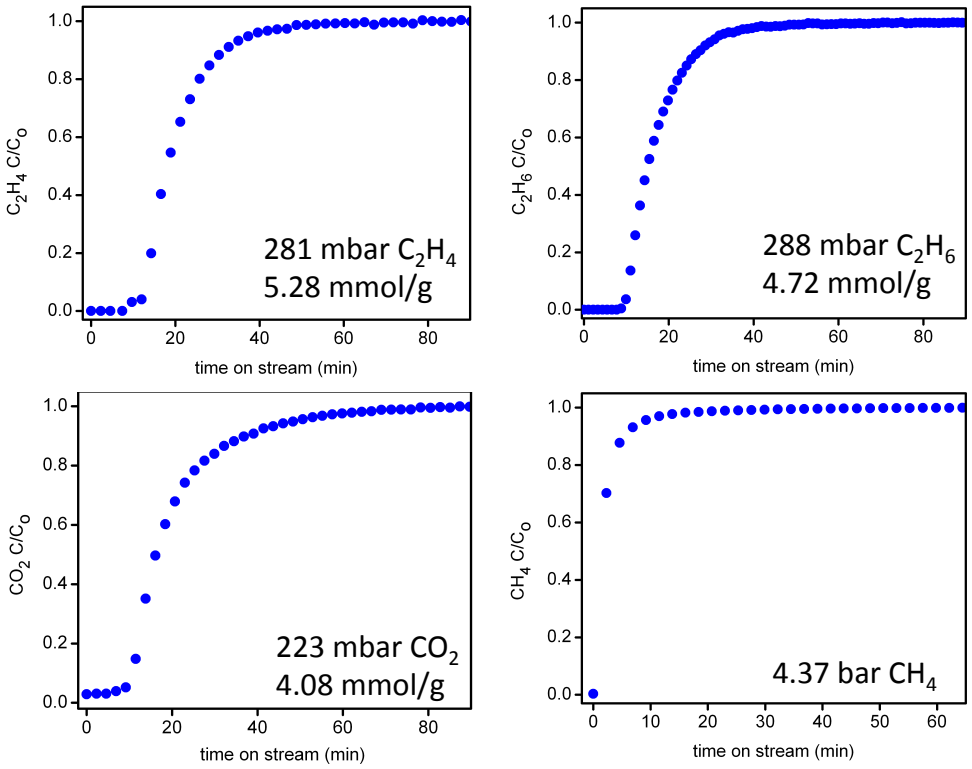

Supplementary Figure 9. Elevated pressure, single-component transient breakthrough curves fpr Mn_2(*m*-dobdc), including the partial pressure of each gas and the corresponding breakthrough capacity. Total pressure is 6.2 bar, with the remainder of the gas being He. Total flow rate is 40 sccm. Temperature is 25 ˚C.

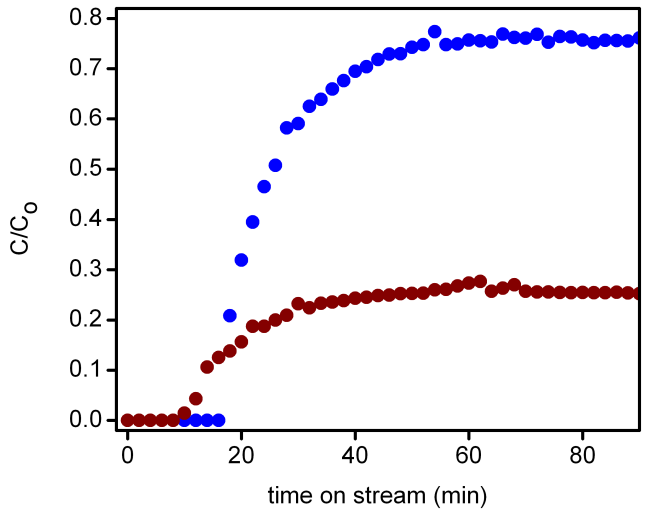

Supplementary Figure 10. Binary transient breakthrough curves of 3:1 ethylene:ethane in Mn_2(*m*-dobdc). Blue and red circles correspond to ethylene and ethane, respectively. Total pressure is 6.2 bar. Total flow rate is 40 sccm. Temperature is 25 ˚C.

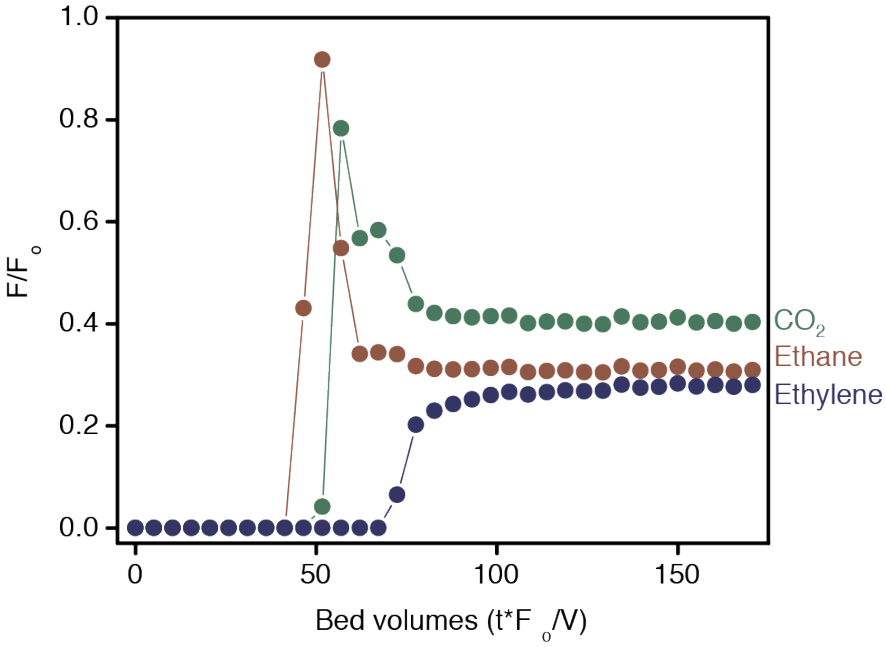

Supplementary Figure 11. Transient breakthrough curve of a CO_2/ethylene/ethane mixture in Mn_2(*m*-dobdc) at a total pressure of 1 bar and 25 ˚C.

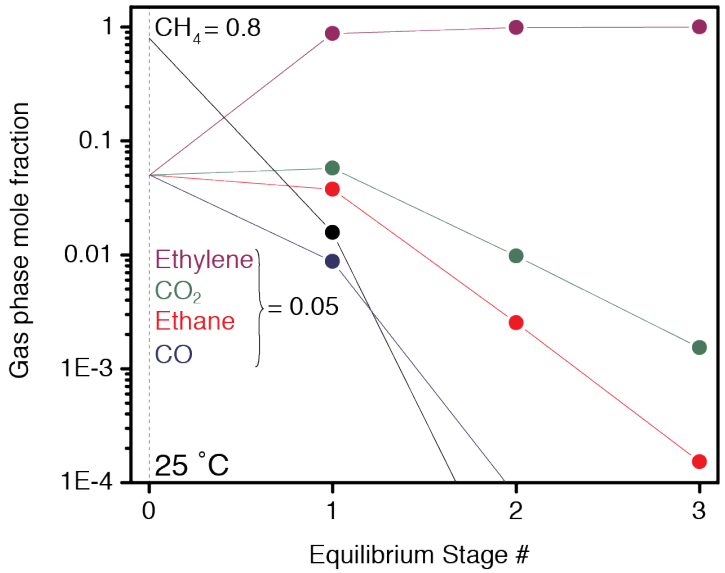

Supplementary Figure 11. 5-Component IAST simulation of an equilibrium stage separation. Initial feed composition, corresponding to stage 0, is 80% CH_4, and 5% of ethylene, ethane, CO_2, and CO. Subsequent equilibrium stage compositions represent the adsorbed phase mole fraction in equilibrium with a gas phase containing the composition from the previous equilibrium stage. After three equilibrium stages, the adsorbed phase is > 99.9% ethylene.

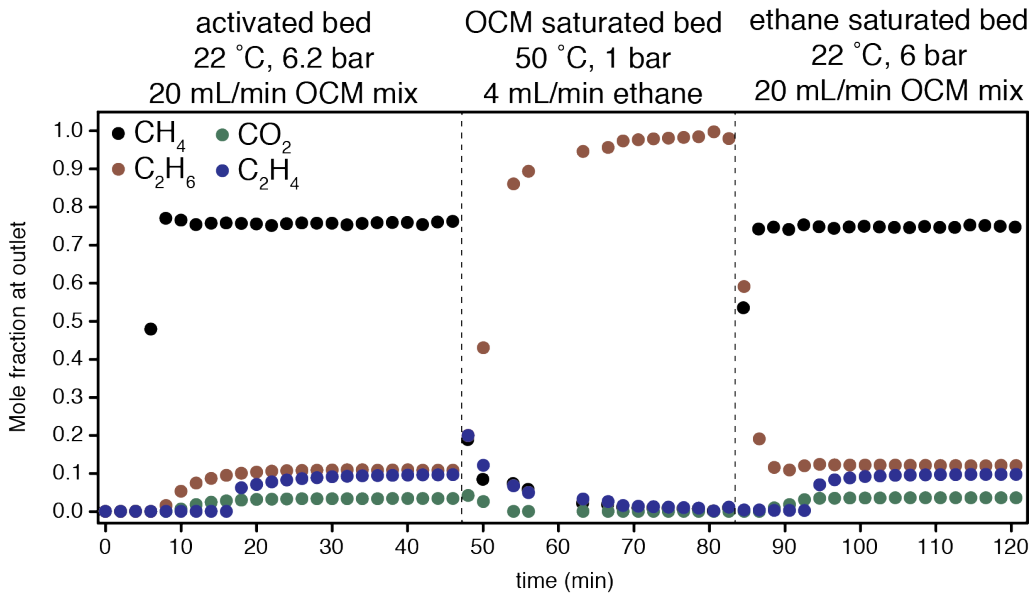

Supplementary Figure 12. Bed cycling experiment using an ethane purge and elevated temperature to regenerate the bed. The experiment is broken into three parts. The first section corresponds to the breakthrough of an OCM effluent gas stream on an activated bed at a total pressure of 6.2 bar and 22 ˚C. The second section corresponds to the gas phase being switched to an ethane purge and the temperature is raised to 50 ˚C. Correspondingly, ethylene and the other adsorbed components are purged from the bed. In the third section, the gas phase was returned to the OCM effluent composition. Ethylene selectivity is maintained after the purge phase.

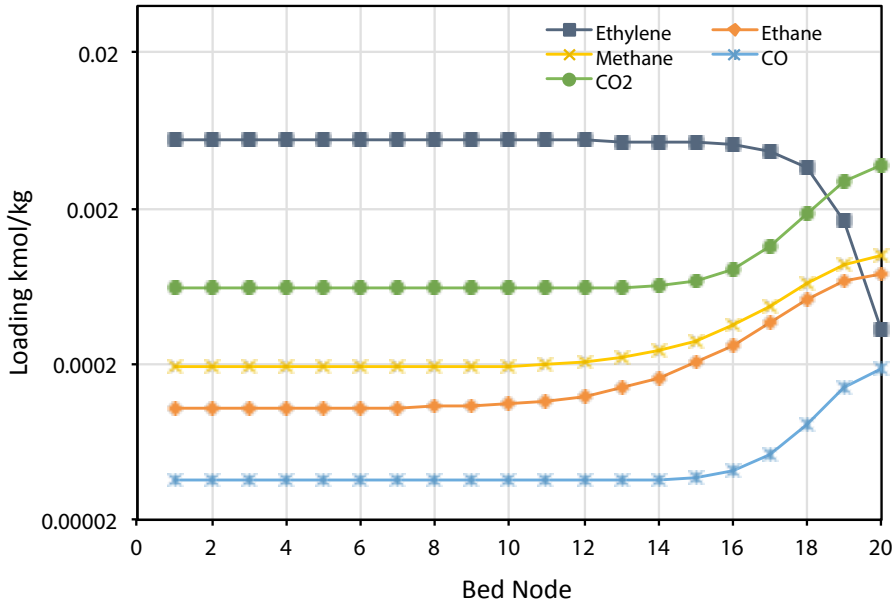

Supplementary Figure 13. Snapshot of the simulated adsorbent bed composition profile following bed saturation with a representative oxidative coupling of methane effluent mixture. The composition is profiled given ethylene recovery threshold of 1000 ppm ethylene at the outlet. The mass transfer zone indicates the portion of the column that is under non-equilibrium conditions. Upstream of the mass transfer zone is under equilibrium conditions. Bed utilization factor is 82%.